

ACTIVE MEDIA

https://doi.org/10.1070/QEL17250

Formation and optical properties of IR photoluminescence centres in bismuth-containing aluminophosphate glass

A.N. Romanov, E.V. Haula, V.N. Korchak

Abstract. **We have prepared aluminophosphate glass samples differing in bismuth oxide content and demonstrating broadband near-IR photoluminescence. Analysis of their photoluminescence spectra leads us to conclude that they contain two main types of emission centres, one of which seems to be a bismuth monocation and the other is a cluster ion. In addition to these luminescence centres, the aluminophosphate glasses contain a nonluminescent bismuth-containing centre responsible for the broad, strong optical absorption band peaking at 450 nm.**

Keywords: *photoluminescence, phosphate glass, subvalent bismuth ions.*

1. Introduction

Found at the beginning of the 21st century, high-intensity broadband near-IR (NIR) photoluminescence (PL) of bismuth-containing SiO_2-based glasses [1, 2] has attracted great interest because the photoluminescence spectrum of such glasses spans the 'telecom window' – the peak transmission range of silica fibre. For this reason, bismuth-containing glasses and crystals are thought to be promising gain media for optical amplifiers and lasers [3]. In a short time interval, researchers found and investigated NIR PL in bismuth-containing phosphate, borate, fluoride, and chloride glasses [4–8] and some halide and oxide crystals [9–18]. The nature of the bismuth-containing centres emitting in the NIR region has long remained unclear, but there is now conclusive experimental evidence that the NIR PL is due to the presence of subvalent bismuth cations, i.e. cations in the oxidation state below the +3 typical of bismuth [6–17, 19]. The likely lasing centre is the Bi^+ monocation. Note that, in SiO_2-based glasses, it can be present, depending on codopants, in various optical centres, such as a Bi^+ $(AlO_{4/2})^-$ ionic centre in aluminosilicate glasses [15, 20] or a covalent bismuth(I) silanolate, ≡SiOBi, in SiO_2 glass without codopants [21, 22]. Bismuth in the oxidation state +1 has rather low chemical stability, so molten glass cooling is accompanied by Bi^+ monocation disproportionation and the formation of clustered bismuth polycations and metallic bismuth nanoclusters [23, 24]. The presence of bismuth clusters and colloids leads to an unwanted optical absorption, so to prevent their formation one has to maintain bismuth concentration in the optical medium at a sufficiently low level. Accordingly, lasing in bismuth-containing glasses has only been achieved at very low bismuth concentrations, and the only type of bismuth laser demonstrated to date is a fibre laser [3], because the low optical gain in it can be compensated for by a large optical path length.

Another interesting feature of bismuth-containing materials (especially of glasses) luminescing in the NIR is that there are several types of emission centres. Whereas bismuth monocation-based NIR PL centres prevail at low bismuth concentrations, raising the bismuth concentration leads to the formation of additional PL centres, which also emit in the NIR [25]. The presence of such additional centres complicates interpretation of PL in bismuth-containing materials and is undesirable from the viewpoint of realising a laser or optical amplifier. The nature of the additional centres is still unclear. Since they are formed at increased bismuth concentrations in materials, they are likely to be clustered subvalent bismuth polycations. Given the practical importance of the formation of various NIR PL centres in bismuth-containing materials, in this work we undertook a systematic study of the photoluminescence and optical absorption of aluminophosphate glass containing different amounts of bismuth from the viewpoint of the formation of multiple photoluminescence and other bismuth-containing centres. Aluminophosphate glass is of interest in that it can contain a large amount of an acid component (P_2O_5): as shown earlier [26, 27], high acidity of the medium is favourable for the stabilisation of subvalent bismuth cations: both mono- and polycations.

2. Experimental

Aluminophosphate glass samples with the initial composition $0.66P_2O_5–0.33Al_2O_3–xBi_2O_3$ (x = 0, 0.01, 0.02, 0.03, and 0.04), containing different amounts of bismuth, were prepared as follows: The 0.44 mole fraction of $Al(PO_3)_3$, 0.11 mole fraction of Al_2O_3, and an appropriate amount of Bi_2O_3 (0–0.04) were thoroughly ground in an agate mortar. The total batch weight was 15 g. The batch was moistened and again ground. The resultant semiliquid slip was loaded into a corundum crucible and heated in air at a constant rate to 200 °C in 1 h and then to 1550 °C in 45 min. After holding at the latter temperature for 30 min, the melt was slowly cooled to room temperature. During cooling, the melt solidified to form transparent coloured glass essentially free of bubbles and other inclusions. The glass did not crack, nor did it detach from the crucible wall. For optical measurements, we prepared 10-mm-thick glass samples having polished plane-parallel faces.

The optical absorption of the samples was measured in the range 400–1000 nm using a Shimadzu UV-3600 UV–Vis–NIR

A.N. Romanov, E.V. Haula, V.N. Korchak N.N. Semenov Federal Research Center for Chemical Physics, Russian Academy of Sciences, ul. Kosygina 4, 119991 Moscow, Russia; e-mail: alexey.romanov@list.ru

Received 4 June 2020
Kvantovaya Elektronika **50** (10) 910–916 (2020)
Translated by O.M. Tsarev

spectrophotometer. NIR photoluminescence spectra (880–1700 nm) were measured on a Solar-LS SDH-IV spectrometer fitted with a Hamamatsu G9204-512S linear InGaAs photodetector array. PL was excited by 50- to 200-mW compact laser modules with wavelengths of 445, 532, 685, and 808 nm. PL excitation spectra were obtained using a tunable light source based on a halogen lamp, an SR540 optical chopper (Stanford Research Systems), and an MDR-206 computer-controlled monochromator (LOMO). Photoluminescence of the samples was detected by an InGaAs photodetector (OAO Polyus). Its signal was fed to an SR830 lock-in amplifier (Stanford Research Systems), together with a reference signal from the optical modulator. After the lock-in amplifier, the signal was sent to an ADC controlled by a computer, where the spectroscopic data were stored. A required PL band was separated out using Thorlabs and Omega Optical interference filters.

The spectra thus obtained were corrected for the spectral sensitivity of the photodetector (PL spectra) and the spectrum of the PL excitation source (PL excitation spectra).

NIR PL decay kinetics were studied at room temperature. The PL was excited by a focused 685- or 808-nm laser diode beam (rectangular 5 μs pulses with a pulse period-to-pulse duration ratio of 1000). After passing through a set of interference filters, which separated out a required spectral band, the PL was collimated to an InGaAs photodetector. Its signal was fed to a preamplifier and then to the input of a PicoScope 5242 digital oscilloscope. To increase the signal-to-noise ratio, the data were averaged over a large number (up to 5×10^4) of measured decay curves. Mathematical processing of the data was performed with software written by us in Fortran using the IMSL Math Library.

3. Results and discussion

The glass samples obtained by us have high transmission and are yellow-brown in colour, with the colour intensity rapidly increasing with bismuth concentration in the glass.

Figure 1 shows normalised photoluminescence spectra of the aluminophosphate glass samples under excitation by laser sources differing in wavelength. It is seen that the PL spectra obtained under excitation at λ = 445, 532, and 685 nm have a strong band peaking at 1100–1180 nm (with the peak position dependent on the PL excitation wavelength) and an extended longer wavelength wing, whose relative intensity rises monotonically with bismuth concentration in the glass. Under excitation at λ = 808 nm, the main PL band is considerably shifted to longer wavelengths and its peak emission wavelength (1270 nm) roughly coincides with the position of the longer wavelength wing in the PL spectra obtained under excitation at 445, 532, and 685 nm. In the PL

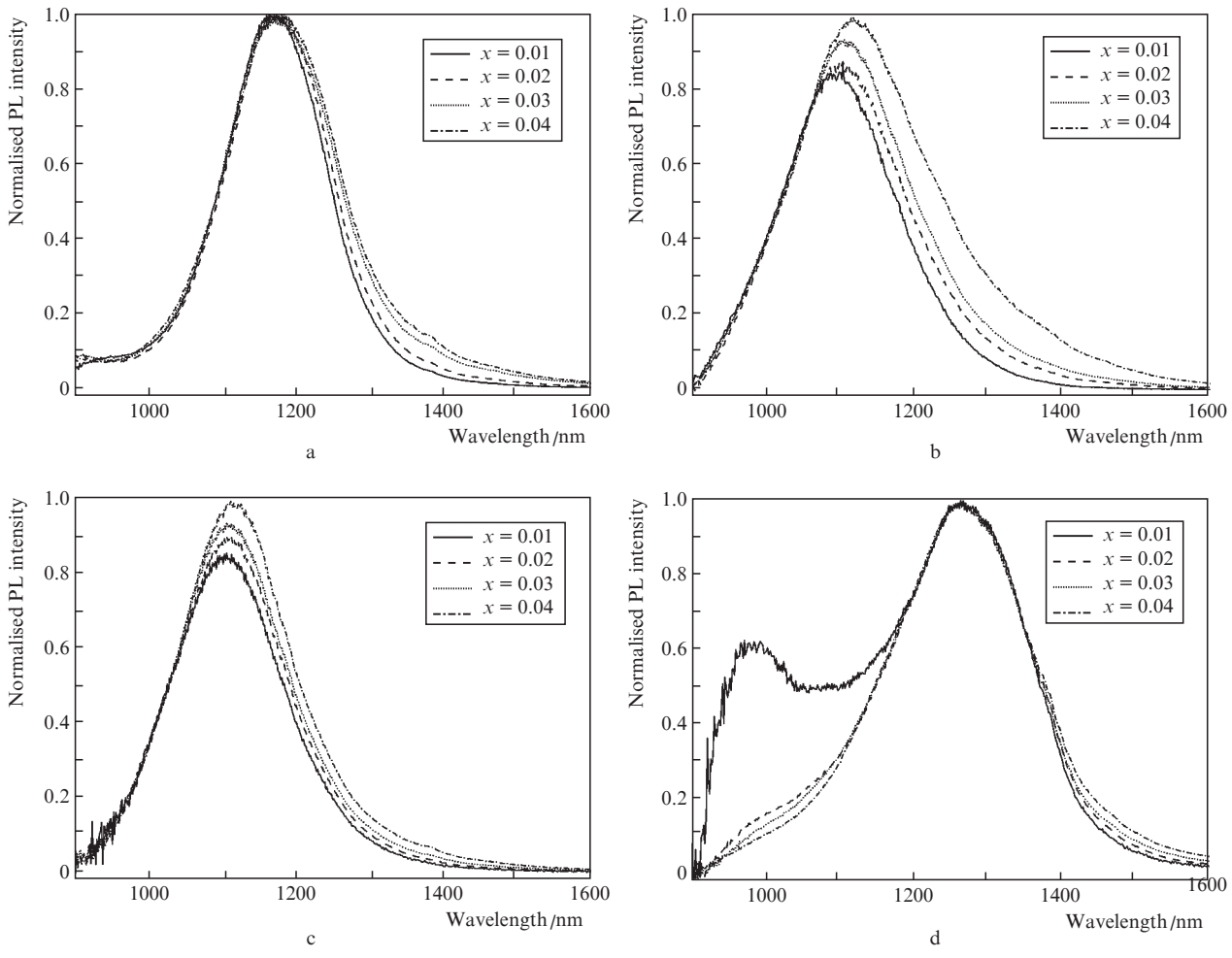

Figure 1. Normalised photoluminescence spectra of the bismuth-containing aluminophosphate glasses with the composition $0.66P_2O_5 - 0.33Al_2O_3 - xBi_2O_3$ (x = 0.01, 0.02, 0.03, and 0.04) under excitation by laser sources at wavelengths λ_{ex} = (a) 445, (b) 532, (c) 685, and (d) 808 nm.

spectra obtained under excitation at 808 nm, the short-wavelength band is also discernible, and its relative intensity decreases with increasing bismuth concentration. The bismuth-free glass sample showed no PL.

These data lead us to assume that there are a few bismuth-containing PL centres in the samples and that the relative concentration of the centres emitting in the longer wavelength wing increases with bismuth concentration. The glass batch contained bismuth in oxide form in the oxidation state +3. Bismuth in this oxidation state is known to have no NIR PL, nor does it absorb light in the visible spectral region [28]. Therefore, the observed NIR PL and colouration of the glass are attributable to the formation of various subvalent bismuth cations during heat treatment of the glass batch and glass formation. In particular, bismuth monocations are formed in a melt at high temperatures through the reduction of trivalent bismuth, $2Bi^{3+} + 2O^{2-} \rightarrow 2Bi^{+} + O_2\uparrow$, accompanied by oxygen gas release. Since the glass was prepared in an ordinary air atmosphere, melt cooling could be accompanied by a reverse reaction – oxidation of the subvalent bismuth cations with atmospheric air – but the rapidly increasing melt viscosity probably prevented this process. This is evidenced by the high spatial uniformity of the colour of the glass samples, whereas without melt stirring the oxidation of the subvalent bismuth cations with atmospheric air leads to bleaching of the glass, predominantly in its surface layer.

The number of different types of bismuth-containing NIR PL centres in our samples can be found with sufficient confidence as described below. Under excitation at a particular wavelength, to each emission centre there corresponds a unique PL spectrum, differing from those of other centres. The PL spectra of different centres can be thought to be linearly independent functions of wavelength. Therefore, at a small optical thickness of a sample, its PL spectrum is a linear combination of N linearly independent components corresponding to N different types of emission centres. Thus, any set of PL spectra corresponding e. g. to an increasing bismuth concentration in the material can be represented by a basis of N orthogonal functions. In experiments, a PL spectrum is determined as a set of intensities (a vector) at k discrete wavelengths $[i(\lambda_1), i(\lambda_2), \ldots, i(\lambda_k)]$. From m such spectra, corresponding to m samples, we can make up an $m \times k$ matrix:

$$\begin{pmatrix} i(\lambda_{11}) & \ldots & i(\lambda_{1m}) \\ \ldots & \ldots & \ldots \\ i(\lambda_{k1}) & \ldots & i(\lambda_{km}) \end{pmatrix}. \quad (1)$$

The rank N of this matrix is equal to the number of linearly independent components necessary for describing a set of m spectra.

Given the presence of noise in experimental data, it is reasonable to evaluate the rank of matrix (1) using singular value decomposition (SVD) [29]. The rank N of the matrix can then be thought to be equal to the number of singular values significantly different from zero, which also corresponds to the sought number of types of emission centres that make a substantial contribution to the emission spectra of the set of samples under consideration.

Figure 2 presents (in the order of decreasing value) the singular values of matrix (1), made up of the PL spectra of four glass samples differing in bismuth concentration under PL excitation at different wavelengths. It is seen that the first three singular values differ considerably, whereas further decrease is not very large. Moreover, the latter two (third and fourth) singular values are rather low and the difference between them is much smaller than in the case of the first, second, and third singular values. It is therefore reasonable to assume that the third and fourth singular values differ from zero only as a result of noise and experimental uncertainties, whereas the former two singular values reflect the actual presence of two linearly independent components whose weighted sum gives the spectra of the samples under study. These data lead us to conclude that the PL spectra of the glass samples under study, differing in bismuth content, are rather well described (with uncertainty down to 1 % judging from the singular values) by a linear combination of two PL spectra corresponding to two different types of bismuth-containing NIR PL centres.

Note that the so-called long-wavelength centre is excited predominantly at $\lambda_{ex} = 808$ nm, whereas the short-wavelength centre is mainly excited at wavelengths of 445, 532, and 685 nm.

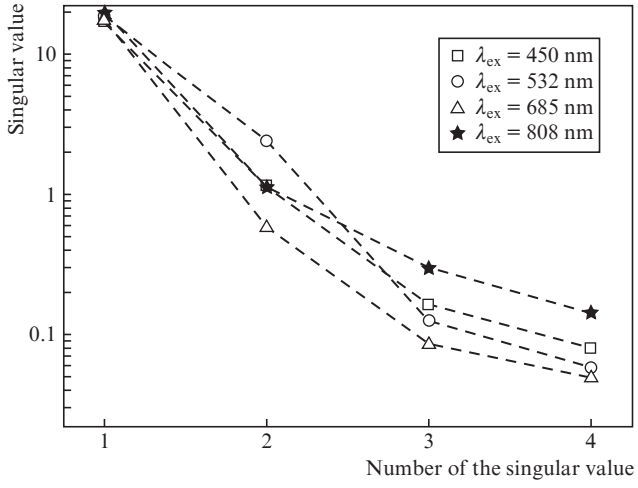

Figure 2. Singular values of matrix (1), made up of the photoluminescence spectra of bismuth-containing aluminophosphate glasses differing in bismuth content under excitation at different wavelengths.

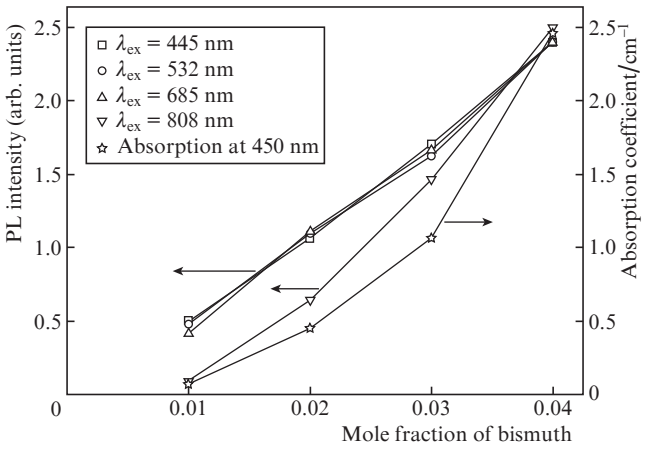

Figure 3. Effect of bismuth content x on the optical absorption at a wavelength of 450 nm and photoluminescence intensity under excitation at different wavelengths (λ_{ex}) in the aluminophosphate glasses with the composition $0.66P_2O_5 - 0.33Al_2O_3 - xBi_2O_3$.

The relative number of long-wavelength centres increases with bismuth concentration in the aluminophosphate glass.

Consider how the PL intensity of the glasses under study varies with bismuth concentration at different PL excitation wavelengths (Fig. 3). As a result, we obtain data predominantly for the long- or short-wavelength centre. Note that the luminescence measurements were made under identical conditions for all the samples. It is seen in Fig. 3 that, upon excitation of the short-wavelength centre at 445, 532, and 685 nm, the PL intensity rises essentially in proportion to bismuth concentration. The slight offset of the lines from the origin can be accounted for in terms of bismuth losses due to vaporisation and adsorption on the crucible wall.

An entirely different dependence on bismuth concentration was exhibited by the PL intensity of the long-wavelength centre under excitation at a wavelength of 808 nm. At low Bi concentrations, there was essentially no PL, whereas increasing the Bi concentration led to a sharp increase in PL intensity, which was obviously nonlinear. Such PL behaviour would be expected upon the formation of clustered bismuth polycations. The formation of clustered bismuth compounds was recently confirmed by direct observation with the use of high-resolution electron microscopy [24].

The short-wavelength centre can, in turn, be identified as a bismuth monocation forming during heat treatment of the glass from trivalent bismuth according to the scheme $2Bi^{3+} + 2O^{2-} \rightarrow 2Bi^{+} + O_2\uparrow$. The intensity of the short-wavelength PL, due to the presence of Bi^{+}, should then be a linear function of the initial Bi^{3+} concentration in the glass batch, as confirmed in our experiments. The other known monatomic bismuth ions either do not emit in the NIR (Bi^{2+} and Bi^{3+}) or are even unstable at high temperatures (Bi^{5+}).

Further insight into the nature of the two emission centres in the glasses under study can be gained from PL excitation spectra measured at emission wavelengths in the range 950–1000 nm, which corresponds mainly to the short-wavelength centre, and in the range 1200–1500 nm, where both centres emit (Fig. 4). It is seen that, in the case of PL measurements in the emission band of the short-wavelength centre, the PL excitation spectrum depends rather little on bismuth concentration in the glass, which is not surprising because another long-wavelength centre, emerging at high bismuth concentrations, makes a negligible contribution to these spectra. The PL excitation spectra consist of two broad bands peaking at 685 and 535 nm. Such PL excitation spectra are characteristic of Bi^{+} monocations and were observed previously in Bi^{+}-containing $KAlSi_2O_6$, $KGaSi_2O_6$, $CsAlSi_2O_6$, and $CsGaGe_2O_6$ crystals [15], zeolite Y [17], and bismuth-containing aluminosilicate glasses [25, 30]. The presence of two bands in the spectrum is due to optical transitions of the Bi^{+} ion between its ground state $^3P_0$ and sublevels of the $^3P_2$ state split by the electrostatic field of the glass host [15].

The PL measurements at emission wavelengths from 1200 to 1500 nm showed that the shape of the spectrum depended significantly on bismuth concentration, because both emission centres contributed to the spectrum, and that features related to the long-wavelength centre prevailed in the spectra of the bismuth-rich samples. At low bismuth concentrations, the spe-

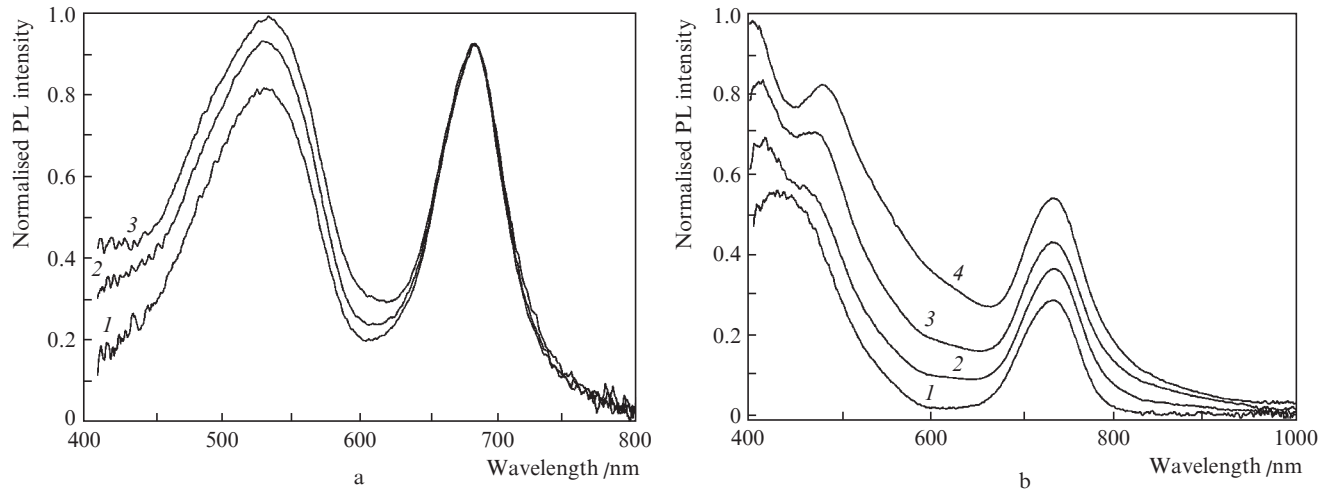

Figure 4. Normalised photoluminescence excitation spectra of the bismuth-containing aluminophosphate glasses with the composition $0.66P_2O_5 - 0.33Al_2O_3 - xBi_2O_3$ at emission wavelengths in the ranges (a) 950–1000 [x = (*1*) 0.02, (*2*) 0.03, (*3*) 0.04] and (b) 1200–1500 nm [x = (*1*) 0.01, (*2*) 0.02, (*3*) 0.03, (*4*) 0.04].

ctrum contained two bands and was attributable to Bi^+ monocations. The peak emission wavelengths of the bands (437 and 737 nm) differ from those in the PL excitation spectrum of Bi^+ at emission wavelengths in the range 950–1100 nm. That the shape of the PL excitation spectrum of bismuth monocations depends on the emission wavelength can be accounted for by the homogeneous broadening of Bi^+ photoluminescence spectra in a disordered glass host [15]. Because of the disorder, Bi^+ cations reside in positions differing in electrostatic field, and the higher the field, the larger are the splitting of the $^3P_1$ and $^3P_2$ excited states and the shift of the PL band to longer wavelengths. Therefore, the PL excitation spectrum measured in the shorter wavelength emission band (950–1100 nm) characterises Bi^+ cations in a weak field, whereas the PL excitation spectrum measured in the longer wavelength band (1200–1500 nm) corresponds to bismuth cations in a strong field. In a strong field, the distance between the two bands in the PL excitation spectrum of Bi^+ is larger and the spectrum approaches that observed for a covalently bonded bismuth(I) silanolate (≡Si–O–Bi) [21]. This is not surprising because covalently bonded Bi^+ cations can be viewed as a limiting case of a strong crystal field.

At high bismuth concentrations, the PL excitation spectra measured in the band 1200–1500 nm are dominated by the contribution from the long-wavelength cluster centre. It is characterised by very broad, overlapping bands peaking at 400 and 490 nm, with the longer wavelength wing of the latter band extending throughout the visible range and into the NIR (λ > 800 nm), where Bi^+ monocations have negligible PL. Because of this, PL excitation at λ_{ex} = 808 nm produces an essentially pure spectrum of the long-wavelength cluster centre (Fig. 1d). The features observed in the PL excitation spectrum of the cluster centre correlate well with those for a Bi_2^+ centre postulated (somewhat arbitrarily) as a long-wavelength emission centre in bismuth-containing aluminosilicate glasses [25]. Since the short-wavelength centre in such glasses is also identified with Bi^+ monocations, it is reasonable to conclude that the bismuth-containing aluminophosphate glasses studied here and the aluminosilicate glasses studied by Veber et al. [25] contain the same types of emission centres. The present data are insufficient to make the final conclusion as to the number of bismuth atoms in the long-wavelength clustered PL centre and its formal charge state, but the assumption made by Veber et al. [25] that this cluster is a dimer is not groundless because, in the case of the aggregation of monatomic ions, it is such centres which are the first to form [24].

The above conclusion that the bismuth-containing aluminophosphate glasses under study contain two different types of NIR PL centres is also supported by our results on PL decay kinetics, which were studied for two $0.66P_2O_5 - 0.33Al_2O_3 - xBi_2O_3$ glass samples, with bismuth concentrations x = 0.02 and 0.04. Pulsed PL excitation was provided by lasers with a wavelength that ensured essentially selective excitation of either Bi^+ monocations (685 nm) or long-wavelength clustered PL centres (808 nm). PL decay was examined in the band between 950 and 1000 nm in the former case and in the band between 1200 and 1500 nm in the case of the cluster centre. The kinetic curves thus obtained are presented in Fig. 5. It is seen that, in the samples differing in bismuth content, the PL decay for the Bi^+ cations is rather well described by the sum of two exponentials having similar parameters [Fig. 5, curves (*1*), (*2*)]. This points to a relatively weak concentration quenching of the excited state responsible for the NIR PL of Bi^+ monocations.

The NIR PL decay of the long-wavelength cluster centre is much faster [Fig. 5, curves (*3*), (4)] than that for Bi^+, and increasing the bismuth concentration in the sample considerably reduces the PL lifetime. In this case, the PL decay kinetics can only be properly described using a stretched exponential model: $I = I_0\exp[(t/\tau)^{0.5}]$. Such kinetics suggest that the excited state involved in PL is depopulated predominantly through nonradiative relaxation such as dipole–dipole energy transfer to some acceptor [31]. The concentration of such acceptor quenchers increases with bismuth concentration in the glass [as evidenced by comparison of curves (*3*) and (*4*)], so the acceptor most likely contains bismuth. Thus, unlike in the case of Bi^+, the PL decay of the long-wavelength cluster centre is mainly due to nonradiative energy transfer processes.

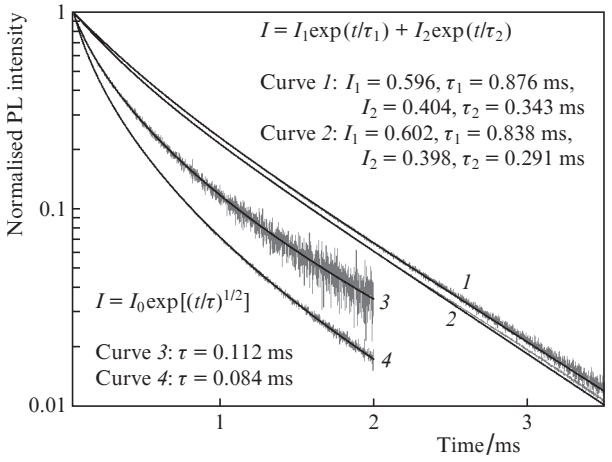

Figure 5. Normalised photoluminescence decay curves of the $0.66P_2O_5 - 0.33Al_2O_3 - xBi_2O_3$ glasses with x = (*1*, *3*) 0.02 and (*2*, *4*) 0.04: (*1*, *2*) excitation by a pulsed laser with λ_{ex} = 685 nm and PL measurements in the band between 950 and 1000 nm; (*3*, *4*) excitation by a laser with λ_{ex} = 808 nm and PL measurements in the band between 1200 and 1500 nm. The solid lines show fits to the experimental data using various model dependences, with the fit parameters indicated.

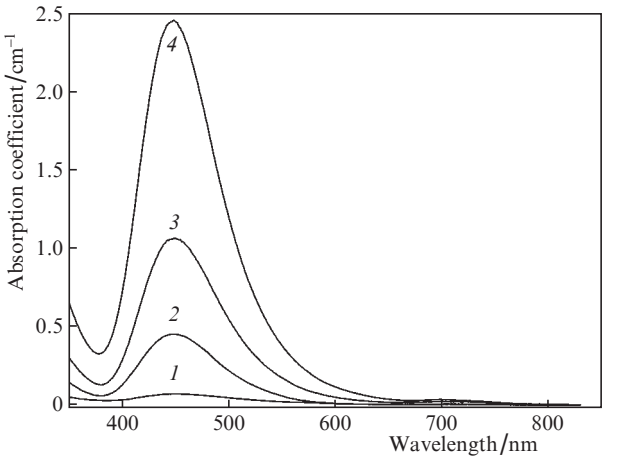

Figure 6. Optical absorption spectra of the bismuth-containing aluminophosphate glasses with the composition $0.66P_2O_5 - 0.33Al_2O_3 - xBi_2O_3$ at x = (*1*) 0.01, (*2*) 0.02, (*3*) 0.03, and (*4*) 0.04.

The optical absorption spectra of the bismuth-containing aluminophosphate glasses under study contain one strong band peaking at 450 nm and a very weak band peaking near 700 nm (Fig. 6). The 700 nm band shows up in the PL excitation spectra as well (Fig. 4) and is attributable to Bi^+ monocations. At the same time, the dominant band at 450 nm has no analogues in position (or in the intensity relative to the 700 nm band) in the PL excitation spectra. The intensity of this band rises nonlinearly and very rapidly with bismuth concentration in the glass, and the variation of the absorption with bismuth concentration does not have any of the features characteristic of the two PL centres (Fig. 3). Therefore, the band peaking at 450 nm, and dominating the optical absorption spectra of the glasses under study, is due to a bismuth-containing centre differing from those responsible for the NIR PL. Note that, judging from the intensity ratio of the optical absorption at 450 and 700 nm, it is the nonluminescent centre absorbing at 450 nm which is the main bismuth-containing centre in the bismuth-rich aluminophosphate glasses.

The nature of this centre is still unclear, but we can draw some conclusions. In particular, the strong dependence of the intensity of the absorption band peaking at 450 nm on bismuth concentration strongly suggests that the corresponding optical centre is a cluster. At the same time, the formation of large colloidal bismuth nanoparticles a few and tens of nanometres in size is unlikely because optical absorption spectra of such particles are well studied [32, 33] and differ from those observed in our experiments (Fig. 6). In the optical absorption spectrum of spherical colloidal bismuth particles, the peak absorption wavelength is near 400 nm and its shift to longer wavelengths can only be caused by the formation of elongated nanoparticles [32], which is unlikely in our experiments. Moreover, increasing the bismuth concentration in a reaction mixture typically leads to an increase in nanoparticle size and, accordingly, to changes in the shape of the optical absorption spectrum. However, with increasing bismuth concentration in our samples the shape of their absorption spectrum remains unchanged (Fig. 6), as does the peak position of the 450 nm band. All this suggests that the absorption band peaking at 450 nm is due to a single type of a bismuth-containing cluster centre with a particular stoichiometry.

4. Conclusions

Bismuth-containing aluminophosphate glasses have been shown to contain two types of NIR PL centres. One of them, a Bi^+ monocation, emits in a band peaking near 1100 to 1180 nm (depending on the excitation wavelength). The other is a clustered bismuth ion (presumably, a dimer) and emits in a band peaking at 1270 nm. The PL decay kinetics of this centre are determined to a considerable degree by nonradiative relaxation processes as a consequence of dipole–dipole energy transfer to some acceptor. In addition to these NIR PL centres, the glasses contain a nonradiative bismuth-containing cluster centre responsible for a strong band peaking at 450 nm in their absorption spectra.

The presence of high concentrations of nonradiative cluster centres and long-wavelength clustered NIR PL centres is undesirable from the viewpoint of obtaining an optical gain due to active Bi^+ centres. There seems to be a few ways to avoid the formation of such cluster centres. First, one can use low bismuth concentrations, as is already the case in fibre lasers. Second, one can use glass with a high glass transition temperature for the higher temperature equilibrium between different subvalent bismuth-containing centres, where there is no aggregation of monatomic bismuth ions or cluster centre formation, to be 'frozen in' during glass cooling. Finally, glass composition should be favourable for bismuth monocation stabilisation.

Acknowledgements. This work was supported by the RF Ministry of Science and Higher Education (state research task, Theme No. V.46.13, 0082-2014-0007, State Registration No. AAAA-A18-118020890105-3).

References

1. Fujimoto Y., Nakatsuka M. *Jpn. J. App. Phys.*, **40**, L279 (2001).
2. Fujimoto Y., Nakatsuka M. *Appl. Phys. Lett.*, **82**, 3325 (2003).
3. Dianov E.M. *Quantum Electron*., **42**, 754 (2012) [*Kvantovaya Elektron.*, **42**, 754 (2012)].
4. Meng X., Qui J., Peng M., Chen D., Zhao Q., Jiang X., Zhu C. *Opt. Express*, **13**, 1628 (2005).
5. Meng X., Qui J., Peng M., Chen D., Zhao Q., Jiang X., Zhu C. *Opt. Express*, **13**, 1635 (2005).
6. Romanov A.N., Fattakhova Z.T., Zhigunov D.M., Korchak V.N., Sulimov V.B. *Opt. Mater.*, **33**, 631 (2011).
7. Romanov A.N., Haula E.V., Fattakhova Z.T., Veber A.A., Tsvetkov V.B., Zhigunov D.M., Korchak V.N., Sulimov V.B. *Opt. Mater.*, **34**, 155 (2011).
8. Romanov A.N., Fattakhova Z.T., Veber A.A., Usovich O.V., Haula E.V., Korchak V.N., Tsvetkov V.B., Trusov L.A., Kazin P.E., Sulimov V.B. *Opt. Express*, **20**, 7212 (2012).
9. Okhrimchuk A.G., Butvina L.N., Dianov E.M., Lichkova N.V., Zagorodnev V.N., Boldyrev K.N. *Opt. Lett.*, **33**, 2182 (2008).
10. Veber A.A., Romanov A.N., Usovich O.V., Fattakhova Z.T., Haula E.V., Korchak V.N., Trusov L.A., Kazin P.E., Sulimov V.B., Tsvetkov V.B. *Appl. Phys. B*, **108**, 733 (2012).
11. Romanov A.N., Veber A.A., Fattakhova Z.T., Usovich O.V., Haula E.V., Trusov L.A., Kazin P.E., Korchak V.N., Tsvetkov V.B., Sulimov V.B. *J. Lumin.*, **134**, 180 (2013).
12. Romanov A.N., Veber A.A., Fattakhova Z.T., Vtyurina D.N., Kouznetsov M.S., Zaramenskikh K.S., Lisitsky I.S., Korchak V.N., Tsvetkov V.B., Sulimov V.B. *J. Lumin.*, **149**, 292 (2014).
13. Veber A.A., Romanov A.N., Usovich O.V., Fattakhova Z.T., Haula E.V., Korchak V.N., Trusov L.A., Kazin P.E., Sulimov V.B., Tsvetkov V.B. *J. Lumin.*, **151**, 247 (2014).
14. Romanov A.N., Veber A.A., Vtyurina D.N., Kouznetsov M.S., Zaramenskikh K.S., Lisitsky I.S., Fattakhova Z.T., Haula E.V., Loiko P.A.,Yumashev K.V., Korchak V.N. *J. Lumin.*, **167**, 371 (2015).
15. Romanov A.N., Veber A.A., Vtyurina D.N., Fattakhova Z.T., Haula E.V., Shashkin D.P., Sulimov V.B., Tsvetkov V.B., Korchak V.N. *J. Mater. Chem. C*, **3**, 3592 (2015).
16. Romanov A.N., Vtyurina D.N., Haula E.V., Shashkin D.P., Pimkin N.A., Kuznetsov M.S., Lisitskii I.S., Korchak V.N. *Khim. Fiz.*, **35** (9), 14 (2016).
17. Sun H.T., Matsushita Y., Sakka Y., Shirahata N., Tanaka M., Katsuya Y., Gao H., Kobayashi K. *J. Am. Chem. Soc.*, **134**, 2918 (2012).
18. Pynenkov A.A., Nischev K.N., Kyashkin V.M., Tomilin O.B., Boyarkina O.V., Firstov S.V. *J. Non-Cryst. Solids*, **480**, 111 (2018).
19. Sun H.T., Sakka Y., Fujii M., Shirahata N., Gao H. *Opt Lett.*, **36**, 100 (2011).
20. Dvoyrin V.V., Mashinsky V.M., Dianov E.M., Umnikov A.A., Yashkov M.V., Guryanov A.N. *Proc. 31st ECOC 2005* (Glasgow, Scotland, 2005) Vol. 4, pp 949–950.
21. Romanov A.N., Haula E.V., Shashkin D.P., Vtyurina D.N., Korchak V.N. *J. Lumin.*, **183**, 233 (2017).
22. Laguta O.V., El Hamzaoui H., Bouazaoui M., Arion V.B., Razdobreev I.M. *Sci. Rep.*, **7**, 3178 (2017).
23. Zlenko A.S., Mashinsky V.M., Iskhakova L.D., Semjonov S.L., Koltashev V.V., Karatun N.M., Dianov E.M. *Opt. Express*, **20**, 23186 (2012).

24. Milovich F.O., Iskhakova L.D., Presniakov M.Yu., Vasiliev A.L., Bondarenko V.I., Sverchkov S.E., Galagan B.I. *J. Non-Cryst. Solids*, **510**, 166 (2019).
25. Veber A., Cicconi M.R., Puri A., de Ligny D. *J. Phys. Chem. C*, **122**, 19777 (2018).
26. Gorodetskii V.V., Shchelkunova N.B., Goncharova E.G., Losev V.V. *Elektrokhimiya*, **12**, 1255 (1976).
27. Bjerrum N.J., Boston C.R., Smith G.P. *Inorg. Chem.*, **6**, 1162 (1967).
28. Runciman W.A. *Proc. Phys. Soc. A*, **68**, 647 (1955).
29. Golub G.H., Van Loan C.F. *Matrix Computations* (Baltimore: John Hopkins University Press, 1996).
30. Firstov S.V., Khopin V.F., Bufetov I.A., Firstova E.G., Guryanov A.N., Dianov E.M. *Opt. Express*, **19**, 19551 (2011).
31. Alekseev N.E., Gapontsev V.P., Zhabotinskii M.E., Kravchenko V.B., Rudnitskii Yu.P. *Lazernye fosfatnye stekla* (Phosphate Laser Glasses) (Moscow: Nauka, 1980).
32. Toudert J., Serna R., de Castro M.J. *J. Phys. Chem. C*, **116**, 20530 (2012).
33. Tian Y., Toudert J. *J. Nanotechnol.*, **2018**, ID 3250932 (2018); https://doi.org/10.1155/2018/3250932.